Electrodynamic Structure of an Outer–Gap Accelerator: Gamma-Ray Emission from the Crab Pulsar

K. Hirotani

National Astronomical Observatory, Mitaka, Tokyo 181-8588, Japan
hirotani@hotaka.mtk.nao.ac.jp

and

S. Shibata

Department of Physics, Yamagata University, Yamagata 990-8560, Japan
shibata@sci.kj.yamagata-u.ac.jp

ABSTRACT

We investigate a stationary pair production cascade in the outer magnetosphere of a spinning neutron star. The charge depletion due to a global current, causes a large electric field along the magnetic field lines. Migratory electrons and/or positrons are accelerated by this field to radiate curvature gamma-rays, some of which collide with the X-rays to materialize as pairs in the gap. The replenished charges partially screen the electric field, which is self-consistently solved together with the distribution functions of particles and gamma-rays. If no current is injected at neither of the boundaries of the accelerator, the gap is located around the so-called null surface, where the local Goldreich-Julian charge density vanishes. However, we first find that the gap position shifts outwards (or inwards) when particles are injected at the inner (or outer) boundary. Applying the theory to the Crab pulsar, we demonstrate that the pulsed TeV flux does not exceed the observational upper limit for moderate infrared photon density and that the gap should be located near to or outside of the null surface so that the observed spectrum of pulsed GeV fluxes may be emitted via curvature process.

Subject headings: gamma-rays: observation – gamma-rays: theory – magnetic field – pulsars: individual (Crab) – X-rays: observation

1. Introduction

The EGRET experiment on the Compton Gamma Ray Observatory has detected pulsed signals from seven rotation-powered pulsars (e.g., for Crab, Nolan et al. 1993, Fierro et al. 1998). The modulation of the γ-ray light curves at GeV energies testifies to the production of γ-ray radiation in the pulsar magnetospheres either at the polar cap (Harding, Tademaru, & Esposito 1978; Daugherty & Harding 1982, 1996; Sturner, Dermer, & Michel 1995; Shibata, Miyazaki, & Takahara 1998), or at the vacuum gaps in the outer magnetosphere (Cheng, Ho, & Ruderman 1986a,b, hereafter CHR; Chiang & Romani 1992, 1994; Romani and Yadigaroglu 1995; Romani 1996; Zhang & Cheng 1997, heafter ZC97). Effective γ-ray production in a pulsar magnetosphere may be extended to the very high energy (VHE) region above 100 GeV as well; however, the predictions of fluxes by the current models of γ-ray pulsars are not sufficiently conclusive (e.g., Cheng 1994). Whether or not the spectra of γ-ray pulsars continue up to the VHE region is a question which remains one of the interesting issues of high-energy astrophysics.

In the VHE region, positive detections of radiation at a high confidence level have been reported from the direction of the Crab pulsar (Nel et al. 1993). However, as for *pulsed* TeV radiation, only the upper limits have been, as a rule, obtained. If the VHE emission originates the pulsar magnetosphere, a significant fraction of them can be expected to show pulsation. Therefore, the lack of *pulsed* TeV emissions provides a severe constraint on the modeling of particle acceleration zones in a pulsar magnetosphere.

In fact, in CHR picture, the magnetosphere should be optically thick for pair–production in order to reduce the TeV flux to an unobserved level by absorption. This in turn requires very high luminosities of infrared photons. However, the required IR fluxes are generally orders of magnitude larger than the observed values (Usov 1994). We are therefore motivated by the need to contrive an outer–gap model which produces less TeV emission with a moderate infrared luminosity.

High-energy emission from a pulsar magnetosphere, in fact, crucially depends on the acceleration electric field, $E_\parallel$, along the magnetic field lines. It was Hirotani and Shibata (1999a,b,c; hereafter Papers I, II, III), and Hirotani (2000a,b,c; hereafter Papers IV, V, VI) who first solved the spatial distribution of $E_\parallel$ to-

gether with particle and γ-ray distribution functions. They demonstrated that a stationary gap is formed around the null surface at which the local Goldreich–Julian charge density,

$$\rho_{\rm GJ} = \frac{\Omega B_z}{2\pi c}, \qquad (1)$$

vanishes, where B_z is the component of the magnetic field along the rotation axis, Ω the angular frequency of the neutron star, and c the speed of light. Equation (1) is valid unless the gap is located close to the light cylinder, of which distance from the rotation axis is given by $\varpi_{\rm LC} = c/\Omega$. In this letter, we develop the method presented in Paper VI, by investigating the case when particles flow into the gap from the inner or the outer boundaries.

In the next two sections, we describe the physical processes of pair production cascade and the resultant γ-ray emission. We then apply the theory to the Crab pulsar and present the expected γ-ray spectra in § 4. In the final section, we compare the results with ZC97.

2. Basic Equations and Boundary Conditions

Let us first consider the Poission equation for the electrostatic potential, Φ. Neglecting relativistic effects, and assuming that typical transfield thickness of the gap, $D_\perp$, is greater than or comparable with the longitudinal gap width, W, we can reduce the Poisson equation into the form (Paper VI)

$$-\frac{d^2}{ds^2}\Phi = 4\pi e(N_+ - N_- - \rho_{\rm GJ}/e), \qquad (2)$$

where N_+ and N_- designate the positronic and electronic densities, respectively, e the magnitude of the charge on an electron, and s the length along the last-open fieldline.

It is convenient to non-dimensionalize the length scales by a typical Debey scale length $c/\omega_{\rm p}$, where

$$\omega_{\rm p} = \sqrt{\frac{4\pi e^2}{m_{\rm e}}\frac{\Omega B_{\rm c}}{2\pi ce}}; \qquad (3)$$

$B_{\rm c}$ represents the magnetic field strength at the gap center. The dimensionless coordinate variable then becomes

$$\xi \equiv (\omega_{\rm p}/c)s. \qquad (4)$$

By using such dimensionless quantities, we can rewrite the Poisson equation into

$$E_\parallel = -\frac{d\varphi}{d\xi}, \qquad (5)$$

$$\frac{dE_{\parallel}}{d\xi} = \frac{B(\xi)}{B_{\rm c}} \left[n_{+}(\xi) - n_{-}(\xi) \right] + \frac{B_z(\xi)}{B_{\rm c}} \qquad (6)$$

where $\varphi(\xi) \equiv e\Phi(s)/(m_{\rm e}c^2)$; the particle densities per unit flux tube are defined by

$$n_{\pm}(\xi) \equiv \frac{2\pi c e}{\Omega} \frac{N_{\pm}(s)}{B(s)}. \qquad (7)$$

We evaluate B_z/B at each point along the last-open field line, by using the Newtonian dipole field.

We next consider the continuity equations for the particles. Assuming that both electrostatic and curvature-radiation-reaction forces cancel out each other, we obtain the following continuity equations

$$\pm B \frac{d}{ds}\left(\frac{N_{\pm}}{B}\right) = \frac{1}{c}\int_0^{\infty} d\epsilon_{\gamma} \left[\eta_{\rm p+}G_+ + \eta_{\rm p-}G_-\right], \quad (8)$$

where $G_{\pm}(s, \epsilon_{\gamma})$ are the distribution functions of γ-ray photons having momentum $\pm m_{\rm e}c\epsilon_{\gamma}$ along the poloidal field line. Since the electric field is assumed to be positive in the gap, e^+'s (or e^-'s) migrate outwards (or inwards). The pair production redistribution functions, $\eta_{\pm}$, are defined as

$$\eta_{\rm p\pm}(\epsilon_{\gamma}) = (1 - \mu_{\rm c}) \frac{c}{\omega_{\rm p}} \int_{\epsilon_{\rm th}}^{\infty} d\epsilon_{\rm x} \frac{dN_{\rm x}}{d\epsilon_{\rm x}} \sigma_{\rm p}(\epsilon_{\gamma}, \epsilon_{\rm x}, \mu_{\rm c}), \quad (9)$$

where $\sigma_{\rm p}$ is the pair-production cross section and $\cos^{-1}\mu_{\rm c}$ refers to the collision angle between the γ-rays and the X-rays (see Paper VI for more details about eq. [9]).

Let us introduce the following dimensionless γ-ray densities in the dimensionless energy interval between β_{i-1} and β_i:

$$g_{\pm}{}^i(\xi) \equiv \frac{2\pi c e}{\Omega B_{\rm c}} \int_{\beta_{i-1}}^{\beta_i} d\epsilon_{\gamma} G_{\pm}(s, \epsilon_{\gamma}). \qquad (10)$$

In this letter, we set $\beta_0 = 10^2$, which corresponds to the lowest γ-ray energy, 51.1 MeV. We divide the γ-ray spectra into 9 energy bins and put $\beta_1 = 10^{2.5}$, $\beta_2 = 10^3$, $\beta_3 = 10^{3.5}$, $\beta_4 = 10^4$, $\beta_5 = 10^{4.5}$, $\beta_6 = 10^{4.75}$, $\beta_7 = 10^5$. $\beta_8 = 10^{5.25}$, and $\beta_9 = 10^{5.5}$.

We can now rewrite equation (8) into

$$\frac{dn_{\pm}}{d\xi} = \pm \frac{B_{\rm c}}{B(\xi)} \sum_{i=1}^{9} [\eta_{\rm p+}{}^i g_+^i(\xi) + \eta_{\rm p-}{}^i g_-^i(\xi)], \quad (11)$$

where $\eta_{\rm p\pm}^i$ are evaluated at the central energy in each bin.

A combination of equations (11) gives the current conservation law,

$$j_{\rm tot} \equiv n_+(\xi) + n_-(\xi) = \text{constant for } \xi. \qquad (12)$$

When $j_{\rm tot} = 1.0$, the current density per unit flux tube equals the Goldreich–Julian value, $\Omega/(2\pi)$.

Unlike the charged particles, γ-rays do not propagate along the local magnetic field lines. However, to avoid complications, we simply assume that the outwardly (or inwardly) propagating γ-rays dilate (or constrict) at the same rate with the magnetic field. This assumption gives a good estimate when $W \ll \varpi_{\rm LC}$ holds. We then obtain (Paper VI)

$$\frac{d}{d\xi} g_{\pm}{}^i(\xi) = \frac{d}{d\xi}(\ln B) \mp \eta_{\rm p\pm}{}^i g_{\pm}{}^i \pm \eta_{\rm c}^i \frac{B(\xi)}{B_{\rm c}} n_{\pm}(\xi), \text{ (13)}$$

where $i = 1, 2, \cdots, m$ $(m = 9)$ and

$$\eta_{\rm c}^i \equiv \frac{\sqrt{3}e^2\Gamma}{\omega_{\rm p}hR_{\rm c}} \int_{\beta_{i-1}/\epsilon_{\rm c}}^{\beta_i/\epsilon_{\rm c}} ds \int_s^{\infty} K_{\frac{5}{3}}(t)dt, \quad (14)$$

where $K_{5/3}$ refers to the modified Bessel function of $5/3$ order.

Equating the electric force $e|d\Phi/dx|$ and the radiation reaction force, we obtain the saturated Lorentz factor at each point as

$$\Gamma_{\rm sat} = \left(\frac{3R_{\rm c}{}^2}{2e}\left|\frac{d\Phi}{dx}\right| + 1\right)^{1/4}; \qquad (15)$$

we compute the curvature radius $R_{\rm c}$ at a point for a Newtonian dipole magnetic field. Since the maximum of $|d\Phi/dx|$ and the potential drop are roughly proportional to W^2 and W^3, respectively (Paper V), the particles become unsaturated for very small W. To avoid an overestimation in such cases, we compute Γ by

$$\frac{1}{\Gamma} = \sqrt{\frac{1}{\Gamma_{\rm sat}{}^2} + \frac{1}{\varphi^2(\xi_2)}}, \qquad (16)$$

where $\varphi(\xi_2)$ represents the maximum attainable Lorentz factor.

2.1. Boundary Conditions

To solve the differential equations (5), (6), (11), and (13), we must impose boundary conditions. At the *inner* (starward) boundary ($\xi = \xi_1$), we impose (Paper VI)

$$E_{\parallel}(\xi_1) = 0, \quad \varphi(\xi_1) = 0, \qquad (17)$$

3

$$g_+{}^i(\xi_1) = 0 \quad (i = 1, 2, \cdots, 9). \tag{18}$$

Since positrons may flow into the gap at $\xi = \xi_1$ as a part of the global current pattern in the magnetosphere, we denote the positronic current per unit flux tube at $\xi = \xi_1$ as

$$n_+(\xi_1) = j_1, \tag{19}$$

which yields (eq. [12])

$$n_-(\xi_1) = j_{\rm tot} - j_1. \tag{20}$$

At the *outer* boundary ($\xi = \xi_2$), we impose

$$E_\parallel(\xi_2) = 0, \quad g_-{}^i(\xi_2) = 0 \quad (i = 1, 2, \cdots, 9), \tag{21}$$

$$n_-(\xi_2) = j_2. \tag{22}$$

The current density created in the gap per unit flux tube can be expressed as

$$j_{\rm gap} = j_{\rm tot} - j_1 - j_2. \tag{23}$$

We adopt $j_{\rm gap}$, j_1, and j_2 as the free parameters.

We have totally 24 boundary conditions (17)–(22) for 22 unknown functions Φ, $E_\parallel$, $n_\pm$, $g_\pm{}^i$ ($i = 1, 2, \cdots, 9$). Thus two extra boundary conditions must be compensated by making the positions of the boundaries ξ_1 and ξ_2 be free. The two free boundaries appear because $E_\parallel = 0$ is imposed at *both* the boundaries and because $j_{\rm gap}$ is externally imposed. In other words, the gap boundaries (ξ_1 and ξ_2) shift, if j_1 and/or j_2 varies.

3. TeV Spectra

For simplicity, assume that the IR field are homogeneous and isotropic within the radius $\varpi_{\rm LC}$. Interpolating the pulsed fluxes in radio, near IR, and optical bands from the Crab pulsar (Moffett and Hankins 1996; Percival et al. 1993; Eikenberry et al. 1997), we obtain (Paper V)

$$\frac{dN_{\rm IR}}{d\epsilon_{\rm IR}} = 1.5 \times 10^{17} d^2 \left(\frac{r_0}{\varpi_{\rm LC}}\right)^{-2} \epsilon_{\rm IR}^{-0.88}, \tag{24}$$

where $\epsilon_{\rm IR} m_e c^2$ refers to the IR photon energy, and $\epsilon_{\rm IR,min} < \epsilon < \epsilon_{\rm IR,max}$. We adopt $\epsilon_{\rm IR,min} = 10^{-6}$ and $\epsilon_{\rm IR,min} = 10^{-2}$; the results do not depend on these cut-off energies very much.

If an electron or a positron is migrating with Lorentz factor $\Gamma \gg 1$ in an isotropic photon field,

it upscatters the soft photons to produce the following number spectrum of γ-rays (Blumenthal & Gould 1970):

$$\frac{d^2 N}{dt d\epsilon_\gamma} = \frac{3}{4}\sigma_{\rm T}\frac{c}{\Gamma^2}\frac{dN_{\rm IR}}{d\epsilon_{\rm IR}}\frac{d\epsilon_{\rm IR}}{\epsilon_{\rm IR}}$$
$$\times \left[2q\ln q + (1 + 2q)(1 - q) + \frac{(Qq)^2(1 - q)}{2(1 + Qq)}\right], \tag{25}$$

where $Q \equiv 4\epsilon_{\rm IR}\Gamma$, $q \equiv \epsilon_\gamma/Q(\Gamma - \epsilon_\gamma)$; $\sigma_{\rm T}$ is the Thomson cross section, and ϵ_γ the energy of the upscattered photons in $m_e c^2$ unit. Substituting equation (24), integrating $d^2 N/dt d\epsilon_\gamma$ over $\epsilon_{\rm IR}$, and multiplying the γ-ray energy ($\epsilon_\gamma m_e c^2$) and the electron number (N_e) in the gap, we obtain the flux density of the upscattered, TeV photons as a function of ϵ_γ.

We finally consider the extrinsic absorption of the TeV photons outside of the gap. For a homogeneous and isotropic IR field, the optical depth becomes

$$\tau(\epsilon_\gamma) = \frac{\varpi_{\rm LC}}{2}\int_{\epsilon_{\rm IR,min}}^{\epsilon_{\rm IR,max}}\frac{dN_{\rm IR}}{d\epsilon_{\rm IR}}\sigma_{\rm p}(\epsilon_{\rm IR}, \epsilon_\gamma, \mu_c)d\epsilon_{\rm IR}, \tag{26}$$

where the path length is assumed to be $\varpi_{\rm LC}/2$.

For the Crab pulsar, $\tau \sim 5$ holds in TeV energies (fig. 1). Therefore, the observed TeV flux reduces to about 1% of the intrinsic flux.

4. Application to the Crab Pulsar

In this section, we apply the theory to the Crab pulsar. The rotational frequency and the magnetic moment are $\Omega = 188.1 \mathrm{rad\,s^{-1}}$ and $\mu = 3.38 \times 10^{30}\mathrm{G\,cm^3}$.

4.1. Electric Field Structure

HEAO 1 observations revealed that the X-ray spectrum in the primary pulse phase is expressed by

$$\frac{dN_{\rm pl}}{d\epsilon_{\rm x}} = N_{\rm pl}\epsilon_{\rm x}^{\alpha} \quad (\epsilon_{\rm min} < \epsilon_{\rm x} < \epsilon_{\rm max}), \tag{27}$$

with $\alpha = -1.81$ and $N_{\rm pl} = 5.3 \times 10^{15}d^2(r_0/\varpi_{\rm LC})^{-2}$ (Knight 1982), where d refers to the distance in kpc. We adopt $\epsilon_{\rm min} = 0.1{\rm keV}/511{\rm keV}$ and $\epsilon_{\rm max} = 50{\rm keV}/511{\rm keV}$. Substituting this power-law spectrum into equation (9), we can solve the Vlasov equations by the method described in § 2.

We consider four representative boundary conditions: We choose $(j_1, j_2) = (0, 0)$, $(0.3, 0)$, $(0.6, 0)$, and $(0, 0.3)$ as cases 1, 2, 3, and 4, respectively. That

is, for case 2 (or case 4), the positronic (or electronic) current density flowing into the gap per unit flux tube at the inner (or outer) boundary is 30% of the typical Goldreich-Julian value, $\Omega/2\pi$. We fix $j_{\text{gap}} = 0.01$ for all the four cases, because the solution forms a 'brim' to disappear (fig. 2 in Hirotani & Okamoto 1998) if j_{gap} exceeds a few percent. In what follows, we adopt $45°$ as the magnetic inclination.

The results of $E_{\parallel}(\xi)$ for the four cases are presented in figure 2. The abscissa designates the distance along the last-open field line and covers the range from the neutron star surface ($s = 0$) to the position where the disance equals $s = 1.2\varpi_{\text{LC}} = 1.91 \times 10^6$ m.

The solid line (case 1) shows that the gap is located around the null surface. However, the gap shifts outwards as j_1 increases, as the dashed (case 2) and dash-dotted (case 3) lines indicate. This result is consistent with what was predicted in Shibata and Hirotani (2000) analytically.

On the other hand, when j_2 increases, the gap shifts inwards and the potential drop, $\Phi(s_2)$, reduces significantly. For example, we obtain $\Phi(s_2) = 7.1 \times 10^{12}$ V for case 4, whereas 1.7×10^{13} V for case 2. The reasons are sixfold: • In a stationary gap, the pair production optical depth, W/λ_{p}, equals the ratio $N_\gamma(j_{\text{gap}}/j_{\text{tot}})$, where λ_{p} and N_γ refer to the pair production mean free path, and the number of γ-rays emitted by a single particle, respectively. • The increased X-ray density at small radii reduces λ_{p}. • The ratio $j_{\text{gap}}/j_{\text{tot}}$ decreases as j_2 increases. • As a result, W decreases very rapidly with increasing j_2. • Owing to the rapidly decreasing W, $\Phi(s_2)$ significantly decreases, although the local ρ_{GJ}, and hence $dE_{\parallel}/ds$ increases at small radii. • As W decreases, N_γ decreases to some extent; however, this effect is passive and cannot change the conclusion.

4.2. Gamma-ray Spectra

The GeV spectra are readily computed from $g_+{}^i(\xi_2)$ and $g_-{}^i(\xi_1)$, while the TeV spectra are obtained by the method described in § 3. We present the γ-ray spectra for the four cases in figure 3, multiplying the cross sectional area of $D_\perp{}^2 = (6W)^2$. If $D_\perp$ increase twice, both the GeV and TeV fluxes increases four times.

In GeV energies, the observational pulsed spectrum is obtained by EGRET observations (filled circles; Nolan et al. 1993), while in TeV energies, only the upper limits are obtained by Whipple observa-
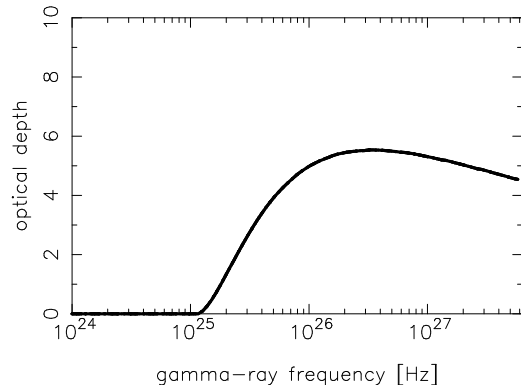

Fig. 1.— Pair production optical depth for a TeV photon to be aborbed in the homogeneous, isotropic IR field in the Crab-pulsar magnetosphere.
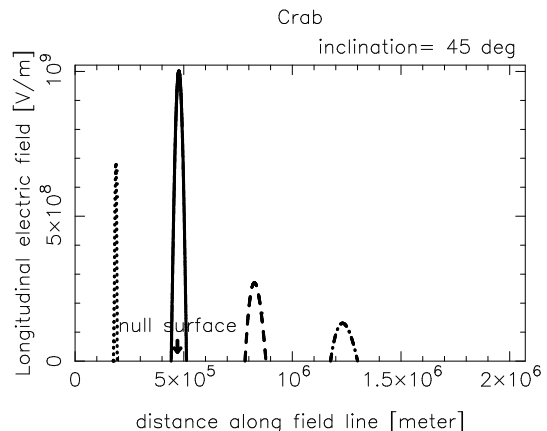

Fig. 2.— Distribution of $E_{\parallel}(\xi)$. The solid, dashed, dash-dotted, and dotted lines correspond to the cases 1, 2, 3, and 4, respectively (see text).

tions (open squares; Weekes et al. 1989; Reynolds et al. 1993; Goret et al. 1993; Lessard et al. 2000), and by Durham observations (open triangle; Dowthwaite et al. 1984). The filled circles denote the unpulsed flux obtained by CANGAROO observations (Tanimori et al. 1998).

The figure shows that the TeV fluxes are kept below the observational upper limits as a whole for appropriate GeV fluxes. Therefore, we can conclude that the problem of the excessive TeV flux does not arise for a reasonable IR density for the Crab pulsar.

It is noteworthy that the GeV spectrum depends on j_1 and j_2 significantly. In particular, in case 4 (as the dotted lines show), the GeV emission significantly decreases and softens, because both the potential drop and the maximum of $E_\parallel$ reduce as the gap shifts inwards. As a result, it becomes impossible to explain the EGRET flux around 10^{24} Hz, if the gap is located well inside of the null surface.

5. Discussion

In summary, we have developed a one-dimensional model for an outer-gap accelerator in the magnetosphere of a rotation-powered pulsar. When the electronic current flows into the gap from the outer boundary, the gap shifts inwards to emit very soft GeV emissions. Applying this method to the Crab pulsar, we find that the gap should be located near to or outside of the null surface, so that the observed spectrum of pulsed GeV fluxes may be emitted via curvature process. By virtue of the absorption by the dense IR field in the magnetosphere, the problem of excessive TeV emission does not arise.

Let us briefly compare the present method with ZC97, who considered that the gap width is limited by the surface X-rays due to the bombardment of the particles produced in the gap. The magnetospheric X-rays considered in this paper is much denser than the surface X-rays due to the bombardment. As a result, the localized gap in the present paper produces less intrinsic TeV flux compared with what would be obtained in ZC97 picture.

For cases 1, 2, and 3, the intrinsic TeV luminosity is comparable or less than the GeV one. Therefore, the Lorentz factors are limited primarily by curvature process (eq.[16]). For case 4, however, the intrinsic TeV luminosity well exceeds the GeV one; therefore, the radiation-reaction forces are due to IC scatterings rather than the curvature process. In fact, we

may expect a sufficient GeV flux via IC scatterings when the gap is located well inside of the null surface. This is because the dense X-ray field will limit the particle Lorentz factors small (Paper II), and because the less-energetic particles scatter copious IR photons into lower γ-ray energies with large cross sections ($\sim \sigma_T$). There is room for further investigation on this issue.

REFERENCES

Berestetskii, V. B., Lifshitz, E. M. & Pitaevskii, L. P., 1989, Quantum Electrodynamics 3rd ed.

Blumenthal, G. R., Gould, R. J. 1970, Rev. Mod. Phys., 42, 237 owden

Cheng, K. S. 1994 in Towards a Major Atmospheric Cerenkov Detector III, Universal Academy Press, Inc., p. 25

Cheng, K. S., Ho, C., Ruderman, M., 1986a ApJ, 300, 500

Cheng, K. S., Ho, C., Ruderman, M., 1986b ApJ, 300, 522

Chiang, J., Romani, R. W. 1992, ApJ, 400, 629

Daugherty, J. K., Harding, A. K. 1982, ApJ, 252, 337

Daugherty, J. K., Harding, A. K. 1996, ApJ, 458, 278

Eikenberry, S. S., Fazio, G. G., Ransom, S. M., Middleditch, J., Kristaian, J., Pennypacker, C. R. 1997, ApJ 477, 465

Harding, A. K., Tademaru, E., Esposito, L. S. 1978, ApJ, 225, 226

Fierro, J. M., Michelson, P. F., Nolan, P. L., Thompson, D. J., 1998, ApJ 494, 734

Hirotani, K. 2000a, MNRAS 317, 225 (Paper IV)

Hirotani, K. 2000b ApJ 545, in press (Paper V)

Hirotani, K. 2000c PASJ 52, 1 (Paper VI)

Hirotani, K. Okamoto, I., 1998, ApJ, 497, 563

Hirotani, K. Shibata, S., 1999a, MNRAS 308, 54 (Paper I)

Hirotani, K. Shibata, S., 1999b, MNRAS 308, 67 (Paper II)

Hirotani, K. Shibata, S., 1999c, PASJ 51, 683 (Paper III)

Hirotani, K. Shibata, S., 2000, submitted to MNRAS

Knight F. K. 1982, ApJ 260, 538

Moffett, D. A., Hankins, T. H. 1996, ApJ 468, 779

Nel, H. I., De Jager, O. C., Raubenheimer, B. C., Brink, C., Meintjes, P. J., Nortt, A. R. 1993, ApJ 418, 836

Nolan, P. L., Arzoumanian, Z., Bertsch, D. L., Chiang, J., Fichtel, C. E., Fierro, J. M., Hartman, R. C., Hunter, S. D., et al. 1993, ApJ 409, 697

Percival, J. W., et al. 1993, ApJ 407, 276

Romani, R. W. 1996, ApJ, 470, 469

Romani, R. W., Yadigaroglu, I. A. ApJ 438, 314

Shibata, S. 1995, MNRAS 276, 537

Shibata, S., Miyazaki, J., Takahara, F. 1998, MNRAS 295, L53

Shibata, S., Hirotani, K. 2000, in preparation

Sturner, S. J., Dermer, C. D., Michel, F. C. 1995, ApJ 445, 736

Thompson, D. J., Bailes, M., Bertsch, D. L., Esposito, J. A., Fichtel, C. E., Harding, A. K., Hartman, R. C., Hunter, S. D. 1996, ApJ 465, 385

Thompson, D. J., Bailes, M., Bertsch, D. L., Cordes, J., D'Amico, N., Esposito, J. A., Finley, J., Hartman, R. C., et al. 1999, ApJ 516, 297

Usov, V. V. 1994, ApJ 427, 394
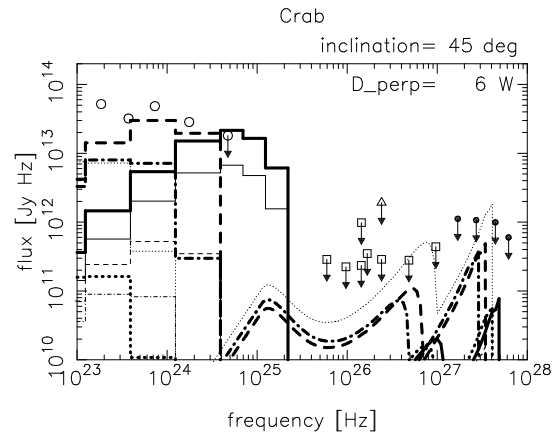
Zhang, L. Cheng, K. S. 1997, ApJ 487, 370

Fig. 3.— Gamma-ray spectra from the Crab pulsar magnetosphere. The thick (or thin) lines represent the flux of outwardly (or inwardly) propagating γ-rays. The solid, dashed, dash-dotted, and dotted lines correspond to the same cases as in figure 2.